Artigo

NON-CRYSTALLINE COPPER OXIDE HIGHLY DISPERSED ON MESOPOROUS ALUMINA: SYNTHESIS, CHARACTERIZATION AND CATALYTIC ACTIVITY IN GLYCEROL CONVERSION TO ACETOL

Tiago Pinheiro Braga[a],*, Nadine Essayem[b] and Antoninho Valentini[c]
[a]Laboratório de Peneiras Moleculares, Universidade Federal do Rio Grande do Norte, 59078-970 Natal – RN, Brasil
[b]Institut de Recherches Sur La Catalyse et L'Environnement, 2 Av. A. Einstein, 69626 Villeurbanne Cedex, France
[c]Departamento de Química Analítica e Físico-Química, Universidade Federal do Ceará, Campus do Pici, 60455-970 Fortaleza – CE, Brasil

Polymeric precursor method and wet impregnation route were applied to synthesize copper and aluminium-based catalysts in order to obtain a material with interesting properties in catalytic reactions. The changes in the structural, morphological and textural properties due to the choice of preparation method were characterized by different techniques, such as XRD, N_2 physisorption isotherms and SEM. The XRD results of the solids present the formation of γ-Al_2O_3 or CuO and β-$Al(OH)_3$, depending on the preparation method. The average crystallite diameters of the alumina were estimated by the Scherrer's formula with a particle size of 5.2 nm. N_2 physisorption isotherms analysis shows that the alumina is a mesoporous material with a high specific surface area. An excessive increase in surface area was observed after Cu^{2+} insertion by wet impregnation from β-$Al(OH)_3$ support, which is explained by the redissolution and recrystallization of bayerite to γ-Al_2O_3 during the impregnation of Cu^{2+} and recalcination process, respectively. The SEM images confirmed this phenomenon. Catalytic tests explain that the combination of the two methods improves the activity, selectivity and the stability in the conversion of glycerol to acetol. The results indicate that the way of catalyst preparation affects its structural, textural and morphological properties and consequently the catalytic performance.

Keywords: copper oxide; alumina; bayerite; glycerol; acetol.

INTRODUCTION

The increasing production of biodiesel has resulted in a price decline of crude glycerol, consequently the utilization of glycerol to produce valuable chemicals, such as 1-hydroxypropan-2-one (acetol) and propylene glycol (1,2-propanediol), becomes an interesting research topic.[1,2] The opportunity exists to market acetol as reduced dyes, food industry (give aroma to foods), flavor compounds in heated milk, skin tanning agent, as well as to produce chemicals such as propylene glycol, propionaldehyde, acetone and furan derivatives.[3-5] Furthermore, acetol is an interesting molecule from astrophysical perspective.[6,7]

The conversion of glycerol to acetol may be conducted via dehydration and/or dehydrogenation reaction.[1,8] Sato *et al.*[1] reported that, for the copper oxide-based catalysts, the major product of glycerol conversion is acetol. The glycerol dehydration proceeds through the formation of Cu-alkoxide species followed by hydrogen abstraction from the secondary hydroxyl groups.[8-10] The alkoxide generated from glycerol may release an OH radical from the primary OH groups to produce acetol. However, copper-alkoxide species may also be produced by interaction with primary hydroxyl groups from glycerol to generate acetol.[8-11] On the other hand, the control of surface acid-base character of support for the copper based-catalysts plays an important role during the glycerol conversion to acetol.[5,8-11]

The most important disadvantage to the gas-phase transformation of glycerol to acetol, mainly on acid catalysts, is the deactivation due to extensive coke deposition on the catalyst surface, as well as the sintering process.[8,12] Therefore, the development of a catalyst resistant to deactivation by coke and the sample sintering during the conversion of glycerol to acetol in gas phase is one of the most interesting research challenges.

Spinels, with the general formula $M^{II}M^{III}_2O_4$, are an important class of oxide materials which have many potential catalytic applications.[13-18] Aluminium based spinels constitute an important group of advanced materials with wide variety of technological applications.[13-19] Copper(II) aluminate, $CuAl_2O_4$, which is known to be an inverse spinel, contains a d^9 metal ion and possesses interesting catalytic properties.[20,21] $CuAl_2O_4$ is formed by solid-solid interaction between CuO and Al_2O_3. Detailed studies on the structure phase of defective copper-alumina (copper-modified alumina) are rarely reported. Furthermore, it was observed that the aluminate spinel may effectively inhibit the coke formation and the thermal sintering.[22] Copper aluminate-like structure (copper-modified alumina) is rarely studied in the glycerol conversion to byproducts,[23] remaining as a largely unexplored research topic.

Braga *et al.*[24] recently showed the synthesis and characterization of different acid supports, $Cu–M_xO_y/Al_2O_3$ (M = Fe, Zn, W or Sb), combined with copper oxide using similar synthetic route and applied in the glycerol conversion to acetol. This study presents the acidity effect of the support and the influence of copper oxide structure on the glycerol catalytic activity. However, the catalytic performance was not presented for the pure aluminium and Cu-Al oxide. Also, the significant increase in surface area of the support after the copper impregnation was not well explained. Thus, further research is needed in order to clarify these points.

Thus, the present study shows the successful method for preparing non-crystalline copper oxide dispersed on mesoporous alumina with a high surface area and the same catalysts are tested in the conversion of glycerol to acetol in gas phase. Despite the importance of transition aluminas for technological and industrial applications, several aspects concerning the chemistry of aluminas, especially combined with other metals such as copper, are still not clear. In this paper, it is presented an unusual change in structural, morphological and textural properties of the alumina with highly dispersed copper oxide prepared using a

*e-mail: tiagoquimicaufrn@gmail.com

combination of two methods (polymeric precursor method and wet impregnation route).

EXPERIMENTAL

Catalyst preparation

This method is based on the chelation of metallic cations (Cu^{2+} and Al^{3+}) by citric acid in a water solution followed by a polyesterification of the remaining carboxylic acid function with ethylene glycol. Aluminum nitrate nonahydrate $\{Al(NO_3)_3 \cdot 9H_2O\}$, copper nitrate trihydrate $\{Cu(NO_3)_2 \cdot 3H_2O\}$, citric acid monohydrate (CA) $\{C_6H_8O_7 \cdot H_2O\}$, and ethylene glycol (EG) $\{C_2H_6O_2\}$ were used as starting chemicals. A CA/metal ratio of 2:1 (mol) was used for all the samples. The metal amount is the sum of Cu and Al. The mass ratio of CA/EG was kept at 2:3. The sample was labeled as XCuAl, with X denoting the Cu/Al weight ratio. The sample containing only aluminum oxide was denominated Al.

For the synthesis process of the 3CuAl sample, where 3 is the Cu/Al weight ratio, Cu and Al salts, respectively, was dissolved in distilled water at room temperature. CA was dissolved in ethanol at 50 ºC. Later, the aqueous solution was added to the CA-ethanol solution and stirred during 60 min at 50 ºC. Subsequently, the EG was added, and the mixture was stirred for 4 h at 100 ºC until it became a viscous resin. The resin was treated at 250 ºC for 1 h under air atmosphere. The resulting precursor composite was ground and treated at 500 ºC under air flow for 2 h. The same conditions were used to prepare Al sample.

Wet impregnation method

Cu dispersed on γ-Al_2O_3 catalyst was prepared by wet impregnation from the aluminium oxide support synthesized by polymeric precursor method (Al sample, as described above) with an aqueous solutions of copper nitrate trihydrate $\{Cu(NO_3)_2 \cdot 3H_2O\}$ in a rotary evaporator. After impregnation, the sample was calcined at 500 °C in muffle furnace for 1 h (5 °C min^{-1}). The sample was denominated XCuAlY, with X representing the Cu/Al weight and Y indicating the calcinations temperature.

Catalyst characterization

The Cu content was determined by ICP after dissolution by acid attack using the line of emission of Cu. The crystal structure of the metal oxides was characterized by X-ray diffraction analysis (XRD), with Cu $K\alpha$ irradiation source (λ = 1.540 Å, 40 kV and 40 mA). Specific surface area (BET) and pore volume of the catalysts were determined by N_2 adsorption/desorption isotherms, at liquid nitrogen temperature. The catalyst samples (80 mg) were vacuum treated at 200 °C for 1 h. The morphology of the catalysts was examined by the use of scanning electron microscopy (SEM) at 20 kV.

Catalytic tests

Catalytic tests were carried out in a fixed bed microreactor, using 200 mg of sample. All fresh catalysts were firstly reduced in H_2 (25 mL min^{-1}) at 250 °C for 1 h. After the temperature of the catalyst bed had been maintained at 250 °C in hydrogen flow for 1 h, an aqueous solution of glycerol at 10 wt.% was fed through the reactor top by a micro-pump at the feed rate of 1.8 cm^3 h^{-1}, which corresponded to 0.06 mol of glycerol *per* hour, combined with a gas (hydrogen) flow rate of 25 mL min^{-1}. The liquid products were collected in an ice-water-salt trap (-6 °C) in order to be analyzed

every hour on a gas chromatograph with a mass spectrometer and a gas chromatograph connected to a hydrogen flame ionization detector (FID-GC), using a capillary column purchased from Varian, CP 9048 (length: 30 m, diameter: 0.32 mm, thickness of the stationary phase: 0.1 mm).

## RESULTS AND DISCUSSION

X-Ray diffraction

The X-ray diffraction patterns are presented in Figure 1. The crystalline phases were identified in comparison with ICDD files. The Al sample is poorly crystalline material and present X-ray patterns of an amorphous solid. However, after multiplying the signal intensity by 4, it is possible to notice some weak broader peaks (18.6, 20.4, 40.6 and 53.3 degrees) related to β-$Al(OH)_3$ phase formation (JCPDS 00-008-0096). On the other hand, the sample 3CuAl clearly pointed out the formation of a copper oxide phase (CuO, JCPDS 04-006-2679) as well as the β-$Al(OH)_3$ phase (JCPDS 00-008-0096).

The samples prepared by wet impregnation (3CuAl500) presented a XRD profile which points to the formation of a material with poorly crystalline organization. In spite of that, the profile suggests the aluminium oxide formation (γ-Al_2O_3, JCPDS 00-002-1414), however, it was not observed crystalline phase of copper oxide, possibly indicating the formation of highly dispersed copper species in alumina matrix.

From this results, one can notice that the samples synthesized by wet impregnation method (3CuAl500) stimulate the formation of aluminium oxide phase with copper oxide highly dispersed compared to the 3CuAl catalyst prepared using only the polymeric precursor method, which show the presence of β-$Al(OH)_3$ and CuO with defined crystallinity.

High dispersed copper oxide phase is probably formed as a result of the thermal solid-state reaction according to the following reaction: $CuO + Al_2O_3 \rightarrow CuAl_xO_y$,[25,26] which indicates that CuO diffused onto the surface of defective spinel-type-γ-Al_2O_3.[27] This suggests that CuO-Al_2O_3 interaction was probably promoted in the samples synthesized by wet impregnation method and it was not possible in the catalyst prepared using only the polymeric precursor method, which presented the formation of copper oxide and hydrated aluminum oxide separately. This phase was not well characterized in any previous literature related to Al_2O_3 and Al-Cu-O system.[28,29] Therefore, in this paper, as previously mentioned,[30] the transition phase was designated Cu-modified γ-Al_2O_3, which the copper is highly dispersed on γ-Al_2O_3, whereas it is not observed defined XRD peaks concerning the crystalline phase of copper oxide. However, for the 3CuAl sample, the isolated CuO phase is not extremely dispersed on the β-$Al(OH)_3$ support, since intense and defined XRD peaks related to copper oxide were observed. Some studies in the literature report that addition of metal ions (M^{n+}) on the support with appropriate pH during the impregnation step catalyzes the transformation of the alumina phase, which can justify the recrystallization of β-$Al(OH)_3$.[31-33]

The average crystallite diameter was estimated from the diffraction data using the Scherrer's formula (Table 1). The average crystallite sizes for alumina particles was 5.2 nm for the sample 3CuAl500. However, the average crystallite size for 3CuAl catalyst was 24.8 nm. The reflections are quite broad for the alumina peaks, indicating the formation of fine nanostructure. Thus, the wet impregnation method from the β-$Al(OH)_3$ synthesized by polymeric precursor method is a successful route for preparing nanometer-sized samples containing alumina combined with a non-crystalline structure of copper oxide (highly dispersed on alumina matrix).
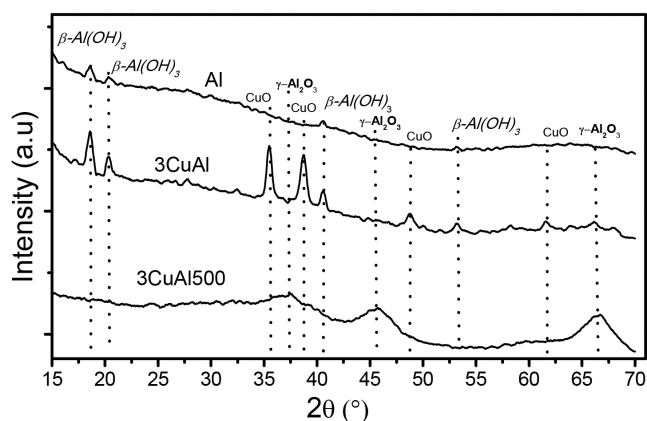
Figure 1. X-Ray diffraction profile of the samples after the calcination. The values were multiplied by 4 for the Al sample. Al: pure alumina by the polymeric precursor method, 3CuAl: copper-aluminium oxide by the polymeric precursor method and 3CuAl500: copper-aluminium oxide by wet impregnation

Table 1. Average crystallite sizes of the solids after calcination process

Samples	crystallite sizes (nm)		
	β-Al(OH)$_3$	CuO	γ-Al$_2$O$_3$
3CuAl	24.2	24.8	-
3CuAl500	-	4.9	5.2

Specific surface area measurements

The nitrogen adsorption/desorption isotherms of the calcined sample prepared from the two method described above are shown in Figure 2 and the textural properties are summarized in Table 2.
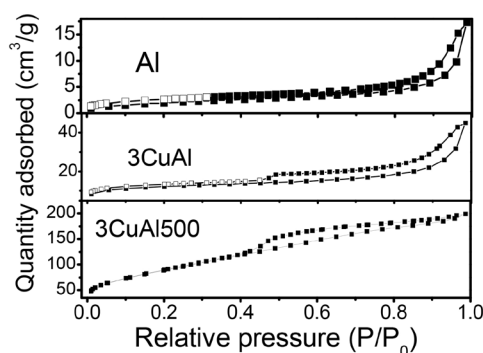
Figure 2. N$_2$ adsorption/desorption isotherms of the catalysts

The samples Al and 3CuAl prepared using only the polymeric precursor method showed analogous isotherm profiles characteristic of mesoporous materials (type II isotherms), which are obtained with aggregates of plate-like particles and therefore possess non-rigid, slit shaped pores. On the other hand, the samples synthesized using wet impregnation method from the β-Al(OH)$_3$ synthesized by polymeric precursor route exhibit a typical type IV curve with H2 hysteresis loops, characteristic of mesoporous materials according to the IUPAC classification. All isotherms display a sharp step typical of capillary condensation of nitrogen within mesopores, where the P/P$_0$ position of the inflection point is correlated to the diameter of the mesopores.

Table 2 lists the surface area (S$_{BET}$), total pore volume (Vp) and average pore diameter (Dp) of solids. It is interesting to note that the specific surface area and the total pore volume of the Al sample prepared by polymeric precursor method increase after the addition

of copper by wet impregnation route. For example, the specific surface area for the Al material compared to the 3CuAl500 catalyst increases from 7 to 328 m^2 g^{-1} and the specific pore volume of the solid also increases from 0.03 to 0.3 cm^3 g^{-1}. Contrary, the sample 3CuAl (41 m^2 g^{-1}) containing mixed copper-aluminum oxide prepared using only the polymeric precursor method indicated that the specific surface area is not extremely different compared to the Al catalyst (7 m^2 g^{-1}) synthesized in the same way.

Table 2. Properties of the samples acquired by N$_2$ adsorption/desorption isotherms

Samples	S$_{BET}$ (m^2/g)	Vp (cm^3/g)	Dp (nm)
Al	7	0.03	15.3
3CuAl	41	0.06	10.6
3CuAl500	328	0.31	3.9

Such textural effects in the porosity of the solids may be related to the information evidenced in the XRD patterns (Figure 1). That is manifested by phase segregation, chemical interactions and polymorphous transformations of the bayerite support (transition of β-Al(OH)$_3$ to γ-Al$_2$O$_3$) during impregnation process. However, the induced increase in the S$_{BET}$ and Vp of the sample prepared by wet impregnation may be also attributed to the creation of pores produced from liberation of nitrogen oxides gas during the thermal decomposition of Cu(NO$_3$)$_2$. Thus, the way of catalyst preparation influences its structure and texture, as observed in Figures 1 and 2, as well as in Tables 1 and 2.

Scanning electron microscopy (SEM)

The morphological features of the sample prepared by two different methods were observed by scanning electron microscopy (Figure 3). The catalysts synthesized using only the polymeric precursor method present a sponge-like morphology, which reveals a high level of porosity. The sponge-like morphology is the result of a thermal decomposition of the organic compounds (CA and EG) and inorganic precursors (nitrates) during the calcination process, which opens channels through the oxide matrix. There are practically no differences between Al and 3CuAl images, as can be seen in Figures 3-a and 3-b.
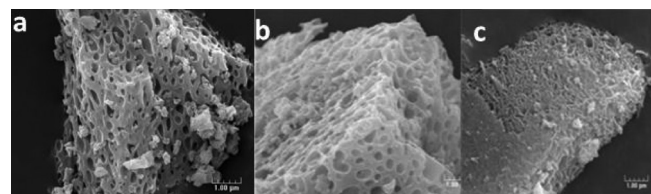
Figure 3. SEM images after the calcinations: a) Al sample; b) 3CuAl catalyst and c) 3CuAl500 solid

On the other hand, the sample 3CuAl500 synthesized using wet impregnation route from the β-Al(OH)$_3$ prepared by polymeric precursor method shows a thin leaf-like morphology (Figure 3-c), which is probably related to the formation of γ-Al$_2$O$_3$ phase, as seen in the XRD pattern (Figure 1). Consequently, the choice of catalyst preparation conditions also influences on the morphology of the catalysts.

These results suggest that probably during the wet impregnation of copper nitrate occurs the redissolution of aluminum hydroxide (β-Al(OH)$_3$), leading to the formation of γ-Al$_2$O$_3$ after calcination at 500 °C. The redissolution followed by recrystallization may explain

the high dispersion obtained for copper oxide, results indicated by X-ray diffraction and the significant increase in surface area and pore volume, as shown in Table 2. It is important to emphasize that the solubility of β-Al(OH)$_3$ in water depends on pH, and the redissolution of the support β-Al(OH)$_3$ can take place in pH=5 (pH of the copper nitrate solution).[22]

It was carried out additional experiments and characterizations in order to confirm that the way to prepare the catalysts leads to a structural transformation and may also lead to a change in the texture of the catalyst (see Figure 3 and Table 2).

Firstly, the sample Al, which showed the formation of β-Al(OH)$_3$, was recalcined at 800 °C under air atmosphere to promote the formation of unhydrated aluminum oxide (Al800). Subsequently, after recalcination at 800 °C, the solid containing aluminum oxide was subjected to the process of wet impregnation for the addition of copper and, finally, the material was calcined again at 500 °C, similar to the route for the preparation of sample 3CuAl500. The sample was designated 3CuAl800, where 3 represents the Cu/Al weight ratio and 800 symbolizes the recalcination temperature of the Al800 support.

It was performed XRD analysis for the two new samples, Al800 and 3CuAl800, to confirm the crystalline phases obtained in the additional experiments (Figure 4). These two materials were compared with the solids Al and 3CuAl500 described previously (Figure 1) to verify the influence of the synthesis process on the obtained structure.
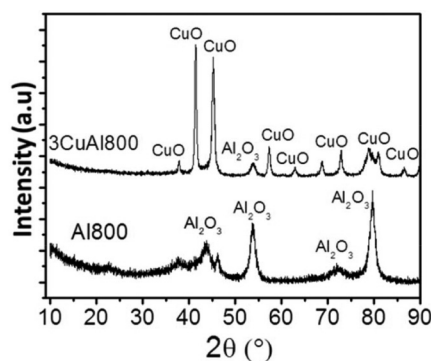

Figure 4. *X-Ray diffraction results of the samples Al800 and 3CuAl800*

From the Figure 4, it was noticed that the sample Al after recalcination at 800 °C exhibited a phase transformation of β-Al(OH)$_3$ to gamma-alumina (γ-Al$_2$O$_3$, JCPDS 00-04-0858). Figure 4 also shows that after addition of copper by wet impregnation from γ-Al$_2$O$_3$ support (Al800), it was observed the formation of copper oxide (CuO, JCPDS 00-003-0867), crystalline phase, besides the gamma-alumina, unlike the catalyst 3CuAl500 which presented the γ-Al$_2$O$_3$ structure with copper oxide (non-crystalline phase) highly dispersed on the support (Figure 1).

Therefore, it is not possible to identify by XRD the formation of copper oxide (isolated CuO phase) for the 3CuAl500 material compared to the solid 3CuAl800. However, in both cases, the calcination temperature employed after copper impregnation of Cu^{2+} was 500 °C, modifying only the crystalline phase of the support ([β-Al(OH)$_3$] for the 3CuAl500 and γ-Al$_2$O$_3$ for the 3CuAl800). Thus, the physicochemical properties of the materials are favored when the impregnation process is carried out using the β-Al(OH)$_3$ support, however, it is not observed when the impregnation has been made with γ-Al$_2$O$_3$ support.

Furthermore, it was also noted that when the copper impregnation has been made from the β-Al(OH)$_3$, the surface area increases by a factor of approximately forty times (Table 2). In order to confirm that the redissolution and recrystallization of β-Al(OH)$_3$ are responsible for the textural changes, the samples Al800 and 3CuAl800 were also analyzed by nitrogen adsorption/desorption isotherms. The result

indicates that the surface area values of the solid Al800 (8 m^2 g^{-1}) was practically the same compared to the support Al (7 m^2 g^{-1}). Thus, the result confirms that the transformation of hydrated alumina (β-Al(OH)$_3$ to γ-Al$_2$O$_3$) using only the polymeric precursor route due to the increase of the calcination temperature without impregnation of Cu^{2+} (from 500 to 800 °C) does not provide an increase in the surface area. Hence, the wet impregnation method is essential for the observed changes in the textural properties due to redissolution and recrystallization of aluminum hydroxide (bayerite).

In addition, the catalyst 3CuAl800 exhibited a specific surface area of 92 m^2 g^{-1}. Therefore, this result indicates that the impregnation of copper nitrate from the support γ-Al$_2$O$_3$ does not lead to a large increase in the surface area compared to the solid 3CuAl500 (328 m^2 g^{-1}), which the impregnation of copper nitrate was carried out from the support β-Al(OH)$_3$.

The persistence of phase β-Al(OH)$_3$ even after the first calcination at 500 °C for Al and 3CuAl samples (Figure 1) may be attributed to the synthesis method employed. The synthetic route chosen uses organic matter (citric acid and ethylene glycol), which undergoes thermal decomposition or elimination. Moreover, Figure 3 shows in microscopic scale that the thermal decomposition and/or elimination process generate pores and the organic material acts as a physical barrier preventing the sintering process of the inorganic fraction during the calcination, justifying the maintenance of the β-Al(OH)$_3$ structure for the Al and 3CuAl samples.

On the other hand, in the recrystallization process at 500 °C (second calcination, after impregnation of Cu^{2+}), it was observed the phase γ-Al$_2$O$_3$ and the absence of phase β-Al(OH)$_3$ due to the fact that the organic material which acts as a physical barrier was completely removed. Thus, in the second calcination process, it was noticed the normal sequence of crystallization for the transition aluminas.

It is known that the pore diameters observed by SEM cannot be compared with the pore diameters obtained from nitrogen adsorption/desorption isotherms. However, Figure 3 suggests that the wet impregnation process of copper nitrate promotes the redissolution of the support β-Al(OH)$_3$, and due to the recalcination step leads to the formation of the phase γ-Al$_2$O$_3$ with high copper dispersion, according to the XRD results (Figure 1).
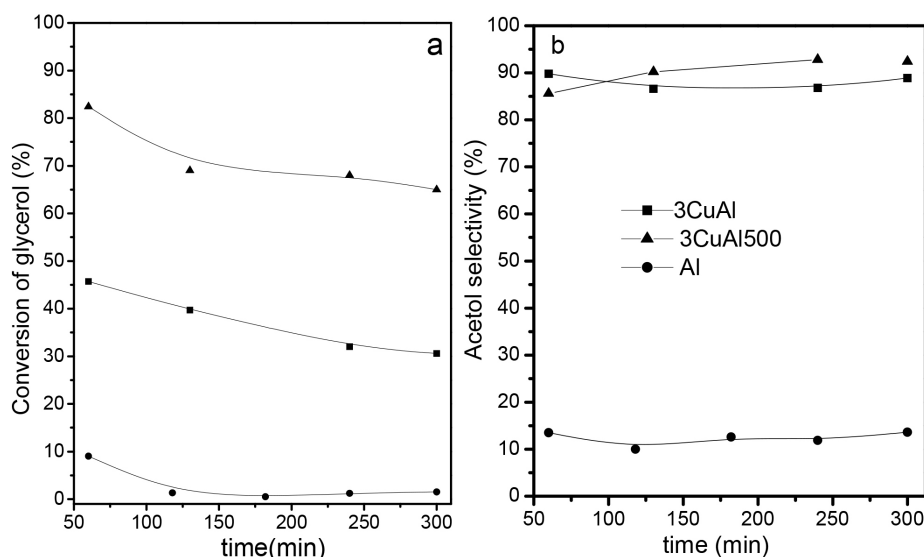
Catalytic activity

The different materials were applied in the gas-phase conversion of glycerol to acetol in order to observe the potential of these solids in catalytic processes. The conversion of glycerol and the acetol selectivity as a function of time for the two different methods is shown in Figure 5.

From Figure 5 is observed that the sample synthesized by wet impregnation method (3CuAl500) presents higher activity and selectivity compared to the 3CuAl catalysts prepared using only the polymeric precursor method. However, the Al sample is almost inactive and less selective for hydroxyacetone, suggesting that the active sites are copper species.

Therefore, the results confirm that the copper is the major active site, while the aluminium oxide plays a secondary role during the conversion of glycerol to acetol. Nevertheless, copper metal sites combined with an aluminium oxide site can play a major role in the activity, selectivity and stability of the samples. Thus, aluminium oxide acts mainly as structural and textural promoter, providing a larger surface area for solids containing copper oxide and aluminium oxide synthesized through wet impregnation route.

From the results presented, one can note that the structural, textural and morphological properties, and consequently the catalytic performance, depend on the way of catalyst preparation due to the fact

Figure 5. *Catalytic performance of the samples: (a) conversion of glycerol, (b) acetol selectivity. Reaction conditions: $T_{reaction}$=250 °C; $T_{reduction}$=250 °C; $m_{catalysts}$=200 mg*

that the sample prepared by wet impregnation presented the gamma-alumina combined with highly dispersed copper oxide containing high surface area and, subsequently, better conversion and stability during the transformation of glycerol to acetol.

The other products selectivity (1,2-propanediol, propanoic acid and acetic acid) is presented in Table 3. For example, the sample 3CuAl presented the 1,2-propanediol, propanoic acid and acetic acid selectivity of 6.0, 4.9 and 0.1%, respectively.

The selectivity results suggest that on the copper surface mainly occur the dehydrogenation reaction, which favor the acetol formation; while the dehydration is promoted by the aluminium oxide.

**Table 3.** Catalytic selectivity observed for others products

Samples	Selectivity (%)*		
	1,2-propanediol	Propanoic acid	Acetic acid
Al	41.7	44.0	1.0
3CuAl	6.0	4.9	0.1
3CuAl500	5.7	1.8	0.06

The spent solids were analyzed by XRD (Figure 6) in order to obtain information concerning the reasons of the decrease in the conversion of glycerol to acetol (Figure 5). The average crystallite sizes were estimated using the Scherrer's formula (see Table 4).

The results presented in Figure 6 for the 3CuAl sample points to Cu^{2+} reduction during the reaction process. The diffraction pattern of the 3CuAl catalyst shows the cuprous oxide formation (Cu_2O, JCPDS 00-003-0867) and metallic copper phase (Cu, JCPDS 00-001-1242).

However, the 3CuAl500 X-ray diffractogram suggests that the structures of aluminium oxide (γ-Al_2O_3, JCPDS 00-002-1414) with copper species highly dispersed was maintained after transformation of glycerol, since it was not observed the formation of crystalline phases of copper during the 4 h reaction period. XRD results of 3CuAl500 catalyst after the reaction (Figure 6) are very similar to the fresh catalyst (Figure 1), which may justify the best catalytic stability compared to the 3CuAl solid.

The average crystallite diameter using the Scherrer's formula for the spent catalysts is shown in Table 4. The metallic Cu was observed in 3CuAl solid after reaction, with a large size of 30.8 nm. On the other hand, the γ-Al_2O_3 phase for the sample 3CuA500 shows high
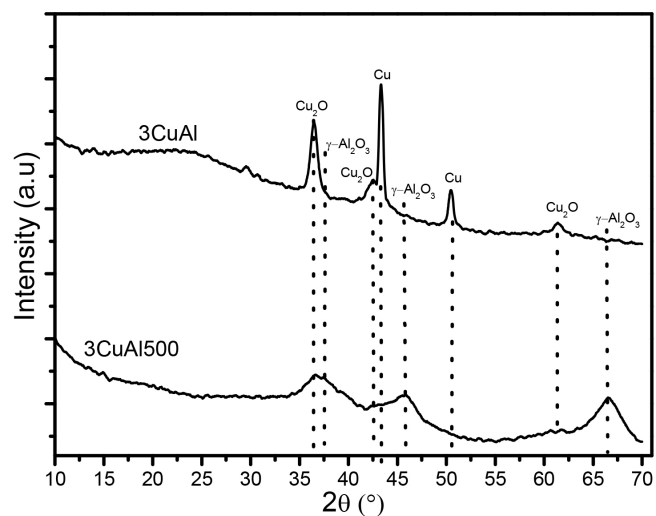
Figure 6. *X-Ray diffraction patterns of the solids after the catalytic test*

Table 4. Average crystallite sizes of the solids for the spent catalysts

Samples	crystallite sizes (nm)			
	Cu_2O	Cu	CuO	γ-Al_2O_3
3CuAl	15.1	30.8	-	-
3CuAl500	6.4	-	4.8	5.9

sintering-resistance ability due to the particle sizes after and before reaction being very similar, as can be observed in Tables 1 and 4. As discussed above, the CuO-Al_2O_3 interaction effect in the samples synthesized by wet impregnation method may be responsible for the sintering-resistant behavior of the catalysts.

CONCLUSION

The wet impregnation method from the β-Al(OH)$_3$ synthesized by polymeric precursor route was applied successfully for the preparation of γ-Al_2O_3 phase containing non-crystalline copper oxide with a high surface area. Copper oxide and alumina-based catalysts were tested in the reaction of glycerol to acetol. The XRD, N_2 adsorption/desorption

isotherms and SEM results showed that the way of catalyst preparation influences its structure, texture, morphology and, subsequently, the catalytic performance. The significant increase of surface area may be justified by redissolution of β-Al(OH)$_3$ during impregnation of Cu^{2+} and recrystallization of bayerite to gamma-alumina during recalcination. The catalyst γ-Al$_2$O$_3$ with highly dispersed copper species achieved the highest catalytic activity compared to the sample containing crystalline copper oxide and bayerite. The presence of γ-Al$_2$O$_3$ interacting with copper oxide provides a lower sintering under reaction conditions.

ACKNOWLEDGMENTS

REFERENCES

1. Sato, S.; Akiyama, M.; Takahashi, R.; Hara, T.; Inui, K.; Yokota, M.; *Appl. Catal. A* **2008**, *347*, 186.

2. Corma, A.; Iborra, S.; Velty, A.; *ChemRev*. **2007**, *107*, 2411.

3. Chiu, C. W.; Dasari, M. A.; Suppes, G. J.; Sutterlin, W. R.; *AIChE J.* **2006**, *52*, 3543.

4. Lacasse, K.; Baumann, W.; *Textile Chemicals Environmental Data and Facts*, 1st ed., Springer: Berlin, **2004**.

5. Mohamad, M. H.; Awang, R.; Yunus, W.; *Am. J. Appl. Sci.* **2011**, *8*, 1135.

6. Jalbout, A. F.; Contreras, F. F.; Adamowicz, L.; *InterScience* **2008**, *108*, 279.

7. Apponi, A. J.; Hoy, J. J.; Halfen, D. T.; Ziurys, L. M.; *Astrophys. J.* **2006**, *652*, 1797.

8. Suprun, W.; Lutecki, M.; Haber, T.; Papp, H.; *J. Mol. Catal. A: Chem.* **2009**, *309*, 71.

9. Li, K. T.; Wang, C.; Wang, H.; *J. Taiwan Inst. Chem. Eng.* **2015**, *52*, 79.

10. Mane, R. B.; Yamaguchi, A.; Malawadkar, A.; *RSC Adv*. **2013**, *3*, 16499.

11. Manfro, R. L.; Souza, M. V. M.; *Catal. Lett.* **2014**, *144*, 867.

12. Miranda, B. C.; Chimentãoa, R. J.; Sueiras, J. E.; *Appl. Catal., B* **2014**, *147*, 464.

13. Wojciechowska, M.; Zielinski, M.; Malczewska, A.; Przystajko, W.; Pietrowski, M.; *Appl. Catal., A* **2006**, *298*, 225.

14. Fortunato, G.; Oswald, H. R.; Reller, A.; *J. Mater. Chem.* **2001**, *11*, 905.

15. Chellam, U.; Xu, Z.; Zeng, H. C.; *Chem. Mater*. **2000**, 12, 650

16. Cui, B.; Lin, H.; Li, J. B.; Li, X.; Yang, J.; Tao, J.; *Adv. Funct. Mater.* **2008**, *18*, 1440.

17. Shchukin, D. G.; Yaremchenko, A. A.; Ferreira, M. G. S.; Kharton, V. V.; *Chem. Mater.* **2005**, *17*, 5124.

18. Ballarini, N.; Cavani, F.; Passeri, S.; Pesaresi, L.; Lee, A. F.; Wilson, K.; *Appl. Catal., A* **2009**, *366*, 184.

19. Giannakas, A. E.; Ladavos, A. K.; Armatas, G. S.; Pomonis, P. J.; *App. Surf. Sci.* **2007**, *253*, 6969.

20. Woelk, H. J.; Hoffmann, B.; Mestl, G.; Schloegl, R.; *J. Am. Ceram. Soc.* **2002**, *85*, 1876.

21. James, T.; Padmanabhan, M.; Warrier, K. G. K.; Sugunan, S.; *Mat. Chem. Phys.* **2007**, *103*, 248

22. Guo, J.; Lou, H.; Zhao, H.; Chai, D.; Zheng, X.; *Appl. Catal., A.* **2004**, *273*, 75.

23. Kwak, B. K.; Park, D. S.; Yun, Y. S.; Yi, J.; *Catal. Commun.* **2012**, *24*, 90.

24. Braga,T. P.; Essayem,N.; Valentini, A.; *RSC Adv.* **2015**, *5*, 93394.

25. Luo, M.; Fang, P.; He, M.; Xie, Y.; *J. Mol. Catal. A: Chem.* **2005**, *239*, 243.

26. Mai, H.; Mengfei, L.; Ping, F.; *J. Rare Earths* **2006**, *24*, 188.

27. Ozawa, M.; Toda, H.; Kato, O.; Suzuki, S.; *Appl. Catal. B:Environ*. **1996**, *8*, 123.

28. Peri, J. B.; *J. Phys. Chem.* **1965**, *69*, 220.

29. Soled, S.; *J. Catal.* **1983**, *81*, 252.

30. Ozawa, M.; Suzuki, S.; Thomas, R. R.; *App. Surf. Sci.* **1997**, *121*, 441.

31. Carrier, X.; Marceau, E.; Lambert, J. F.; Che, M.; *J. Colloid Interface Sci.* **2007**, *308*, 429.

32. Trueba, M.; Trasatti, S. P.; *Eur. J. Inorg. Chem.* **2005**, *17*, 3393.

33. Maity, S.; James, O. O.; Chowdhury, B.; Auroux, A.; *Curr Sci.* **2014**, *106*, 1538.